JOURNAL OF ENVIRONMENTAL HYDROLOGY

Open Access Online Journal of the International Association for Environmental Hydrology

VOLUME 27 2019

INFLUENCE OF LAND USE AND GEOMORPHOLOGY ON THE FLOW OF THE PINDO RIVER, ECUADOR

Ricardo Abril[1]
Yenny Yanez[2]
Carolina Villarroel[3]
Iván Idrovo[1]
Edgar Caicedo[1]
Mayra Vargas[4]
André Tapia[5]
Mariela Valle[1]

[1]Universidad Estatal Amazónica, Departamento de Ciencias de la Vida, Ecuador
[2]Unidad Educativa Intercultural Bilingüe Luis Felipe Wajerei Shushufindi, Sucumbios, Ecuador
[3]Unidad Educativa Intercultural Bilingüe San José de Chonta Punta Tena, Napo, Ecuador
[4]Constructora CYSCONSEROIL Joya de los Sachas, Orellana, Ecuador
[5]Gobierno Autónomo Descentralizado Provincial de Pastaza, Programa de Educación Ambiental. Pastaza, Ecuador

This study has been carried out in the upper basin of the Pindo River and its tributaries, province of Pastaza, Ecuador. Geomorphological variables coverage and infiltration velocity, flow and precipitation was recorded for 12 months.(Jul 2017- Jul 2018). The objective of this research was to determine the influence of the geomorphological and edaphic characteristics on the flow variability of the upper Pindo river basin. The correlation coefficient was determined; The variance analysis between the variables, the IDF curves at a return period of 2 and 5 years, and the synthetic hydrograms have been analyzed. These have been compared with the records of the last flood, with and without loss, with the flow registered throughout the water footprint. The recharge areas have been located between 2.77 and 6.95 km^2, with concentration times between 0.50 and 0.90 hours and compactness coefficients between 1.16 and 1.75. Land uses of forest soil, pasture, enhancement and mosaic have been identified. The reported infiltration rate value was lower than 60 cm/h. The highest flows have been reported in the Pindo river at the "metallic bridge" point and in the Charguayacu and Bravo tributaries. The correlation analysis has showed significant values at 0.05: negative regarding velocity and 2-hours cumulative infiltration, positive regarding compactness coefficient and 5-days previous rainfall; positive at 0.01 regarding the area and negative regarding the drainage density. Within the unit hydrograph model without loss, the flow has been estimated with the water footprint method. It has been concluded that the flow is influenced by the morphological characteristics, coefficient of variation, and the meteorology. The land use influences the flow infiltration and variability.

INTRODUCTION

River basin runoff can change due to variations in precipitation, infiltration and evapotranspiration. Changes in land use can affect the flow by increasing or decreasing runoff (Ren et al., 2014). Vegetation cover influences these hydrological processes in a complex way. Its increase in hydrological basins shows, in a general way, the decrease of surface runoff by increasing the infiltration capacity of soils, as well as the effect generated by the vegetation cover in evaporation, interception and redistribution of precipitation (Pérez et al., 2018). In this regard, Villavicencio et al., (2014) proposed a forest ecosystems act as hydric sponge since they reduce the winter time flows and maintain them during summer time

The mathematical model allows to study the distinct phenomena which occur in a basin simplifying and representing its different inherent characters. These mathematical models are important tools which have been improved throughout time (Pizarro et al., 2005). The methods used to estimate the influence of geomorphology on the river attributes are not meant of large rivers (Helton et al., 2014), hence in the present study it is compared with small rivers which are homogenous in nature.

The soil, through its infiltration capacity, regulates water balance by absorbing precipitation and is affected in intensively used soils (Argañaraz and Lorenz, 2010). The surface currents are influenced by the geomorphology, hydrogeology and climate conditions. Simulation models used to observe the response of a water body contemplate the geometry and hydrological conditions. (Sun et al., 2016). The recharge areas are important since they are the main sources of drinking water supply, and play a very important role within the water cycle.

Torrential floods generate greater damage due to their rapid occurrence, violence and the dragging of coarse sediments in contrast to floods, where water slowly overflows its channel only with suspended materials (Garzón et al., 2009). Therefore, knowing the flood zones is fundamental in the design of infrastructures. (Conesa & García, 2011a). In this aspect, sudden avenues, which differ from floods, constitute one of the processes with the greatest generation of risks for areas near watercourses. (Aroca, E. 2014). Geospatial programs and hydrological calculation engines such as HEC-HMS and HEC-RAS are used in order to model the rainfall-runoff relationships (Conesa & García, 2011b). These elements hypothesize that geomorphological characteristics and land use influence surface flow regimes.

The objective of this research work was to determinate the influence of the geomorphological and edaphic characteristics on the flow variability of the upper Pindo river Basin.

MATERIALS AND METHODS

This study took place in the high area of the Pindo river sub-basin, considering the following water bodies: the upper area of Pindo river, “collecting point”, “metallic bridge”, “unnamed tributary”; the “Charguayacu” river at the bridge and its mouth and the “Plata” and “Bravo” rivers which are located in the Pastaza province in Ecuador. The characteristics and coordinates using the WGS84 system in the area 17 S are shown in the Figure 1.

Edaphoclimatic features

Soils are classified as Hydrandepts which is typified by a loamy texture, deep and totally leached, they have a dark-brown color, poor in phosphor and potassium, the pH is strong to moderately acid between 4,9-5,9 (Abril, 2012). Regarding the meteorological characteristics, this area has an average temperature of 22.6 °C, and a relative humidity of 84% (Abril 2012). Table 1 shows the average

precipitation values for the period 1981-2018 extracted from the data base of the meteorological station of Amazonas River Airport where a downward trend is observed which happens to be also a trend over the last five years with averages of: 5707.22 (1981-1985), 5605.4 (1986-1990), 5477.36 (1991-1995), 5197.28 (1996-2005), 5341.52 (2001-2005), 5006.82 (2006-2010), 5156.72 (2011-2015).

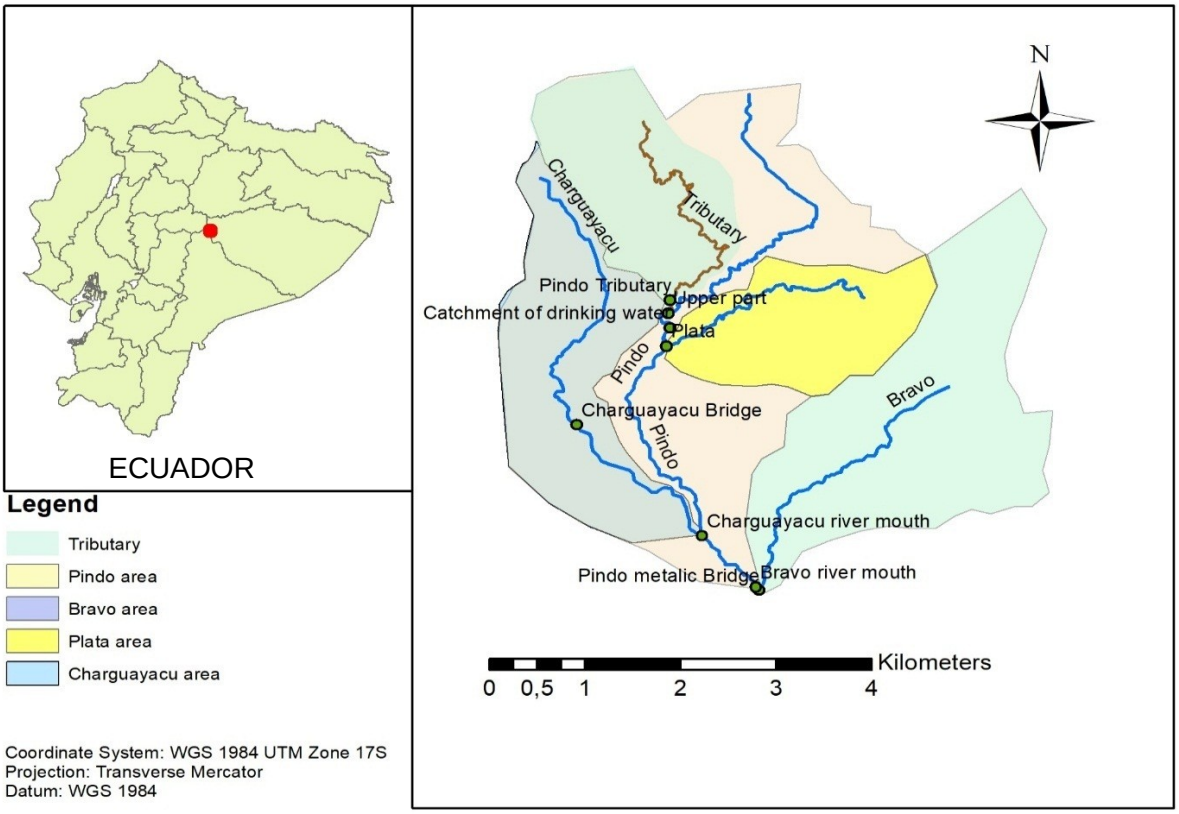

Figure 1. Location study area and monitoring points

Table 1. Precipitation data of Rio Amazonas Airport meteorological station

Monthly average precipitation (mm)													
	Jan	Feb	Mar	Apr	May	Jun	Jul	Ago	Sep	Oct	Nov	Dec	Total
Aver.	421.3	394.9	443.3	567.2	528.7	512.8	398.6	335.3	366.8	478.0	470.6	450.0	5367,4
Max	825.5	666.7	657.6	885.7	959.6	861.2	719.9	555.4	604.3	769.9	650.6	694.7	6270,6
Min	213.9	113.1	244.5	160.3	291.6	297.1	239.7	115.2	177.3	270.1	268.5	270.5	4351,5
Year cumulative precipitation (mm)													
Year	1981	1982	1983	1984	1985	1986	1987	1988	1989	1990	1991	1992	1993
	5736.2	6161.4	5732.1	5639.7	5266.7	6154.5	5257.6	4718.6	5625.7	6270.6	5635.8	5014.9	6197
Year	1994	1995	1996	1997	1998	1999	2000	2001	2002	2003	2004	2005	2006
	5739.2	4799.9	5267.2	4913.1	4863.1	5259.5	5683.5	5115.7	5182.9	5344.3	5755.3	5309.4	4841,8
Year	2007	2008	2009	2010	2011	2012	2013	2014	2015	2016	2017		
	5641	5121,4	5078,4	4351,5	4684,7	4891	5480,6	5015,6	5711,7	5281,1	5850,6		

Delimitation of recharge areas of watercourses

A route has been made along the watercourses identifying the spots using a GARMIN GPS, Google Earth Pro and QGIS programs and the geospatial base information. The recharge zones have been delimited following the watershed (Ruiz & Torres 2008). The main irrigation channel has been

established based on the largest drainage area following the proposal made by Ruiz & Torres (2008). The partial and accumulated distance of the irrigation channel course has been determined establishing the slope corresponding to each sampling spot whereupon the concentration times were estimated through the Kirpich equation (Gaspari et al., 2013) (Equation 1), the relative parameters of the basin´s shape, as a compactness coefficient or Graveolus index (Equation 2), the relation of elongation (Breña, 2006) (Equation 3), the drainage density (Equation 4) (Meza, et al., 2014) and the current density (Equation 5) (Breña, 2006)

$$Tc = [\![0.06628L]\!]^{0.77} / S^{0.385} \quad (1)$$

where Tc = concentration time (hrs), L = channel length (km), and S = slope.

$$Kc = (0.28 * P) / (\sqrt{A}) \quad (2)$$

$$Re = (1.128\sqrt{A}/Lc) \quad (3)$$

$$Dd = (\Sigma Lc) / A \quad (4)$$

$$Dc = Nc / A \quad (5)$$

where Kc = coefficient of compactness, Re = relation of elongation, Dd = drainage density, Dc = current dentsity, P = perimeter of the basin, A = area of the basin, Lc = length of the irrigation channel (river bed), and Nc = number of currents.

Parameters related to infiltration have been determined. This was carried out in three different spots on both sides of the irrigation channel in each water course, before it merged with another water course. This method was applied to determine the basic velocity of vertical soil infiltration. In order to do this, a cylinder was introduced into the soil covering from 15 cm to 10 cm depth, then it was filled up with water until it reached the same level (Blanco, 1999). For the data analysis, the average infiltration velocities (Equation 6) at 60 and 120 minutes. In the infiltration phase, the tests were carried out in three zones on both sides of the river (right and left), taking into account the vegetation cover and the type of soil.

$$VI\ prom = Iacum / t \quad (6)$$

where VI prom = average infiltration rate, Iacum = accumulated infiltration, T = time

The determination of the water flow was made using the Maning formula (Equation 7), (Colmenares et al., 2013). The coefficient of roughness was determined with Equation 8 (Bray Equation (Bray 1979).

$$V = (R^{2/3} S^{1/2}) / n \quad (7)$$

where V = average speed of the current (m/s), R = hydraulic radius (m), S = average channel slope (m/m), n = Manning roughness coefficient,

$$n = 0.0495 * (\text{stones diameter})^{0.16}. \quad (8)$$

The SCS unit hydrograph method was applied to estimate the flood flow. To calculate the response time, the CN curve number method was applied, which can be applied to basins larger than 16 km^2. It is performed based on rainfall and run-off data during a 24 hours lapse. Therefore the calculation of the Effective Precipitation is limited, since it does not consider temporal variations in rainfall intensity (Gaspary et al., 2013).

The Pearson R^2 correlation coefficient was determined between the variables using the SPSS software (IBM, 2013), the variance analysis of the infiltration rate and coefficient of caudal variation

with the Duncan´s mean comparison test between coverage groups. The variation coefficient of the flow rate was determined as a function of the type of soil cover variable, while for the coefficient of flow variation variable, the variables of average infiltration speed at 60 and 120 min were considered.

The meteorological information of the weather station located at the "Rio Amazonas Airport" from 1981 to 2017 of which the rainfall records are available (max/24h) has been reviewed. The rain gauge station located at the "Pindo mirador" biological station was also taken into consideration this was recorded data per hour from 2014 to 2018. Based on this information, it has been determined which have been the maximum values historically reported for 24h.

The modeling of the flood flows was made considering the precipitation records per hour on December 30th, 2016. On that day, the highest rainfall in the area was reported. The modeling was carried out applying the SCS hydrograph methodology for each watercourses individually. The modeling of all water courses was also conducted using the HEC-HMS program(U.S. Army Corps of Engineers, 2017). These flows were compared with those estimated through the water footprint method recorded in the flood event on that day.

RESULTS

The hydrographic and geographic characteristics shown in Table 2 indicate that the recharge areas for the zone correspond in their entirety to very small basins, where the smaller tributaries areas correspond to the tributary of the Pindo River. The collecting point collects the flows of the upper Pindo and tributary courses, while the metallic bridge area incorporates the flows of the "Plata" and "Charguayacu" watercourses.

Pindo is considered the main river because it shows the largest recharge area. It also presents the largest concentration time in the area according to the characterization of Chow et al. (2013). On the other side, the metallic bridge area of the river is characterized by mountains with slopes greater than 7%. By joining the recharge areas, the union of the different branches leads the Pindo River to have the highest drainage density.

The cumulative infiltration (Figure 2) was taken at 3 spots in each course. It reported higher values at 1 and 2 hours in plot 3 on the right riverside of the Pindo river watercourse with values that exceeded 100 cm, whereas Río Plata had the lowest values with 1.8 and 3.6 cm respectively.

Table 3 shows the values of the infiltration velocity (cm/h) where Rio Pindo reports the highest average for both, the 1h and 2h measurements, but this one also reports a greater variability as reported by the values of the standard deviation and the coefficient of variation. The lowest values in terms of the average at 1 and 2h have been reported by the unnamed tributary, whereas the lowest variability has been observed in the Charguayacu river. This findings indicate the greater heterogeneous conditions within the area. In the unnamed tributary, the average infiltration was 10 mm/h, with values ranging between 2.5 and 43.3 cm/h.

The flows registered in Pindo River (Figure 3A) show higher volumes in the metallic bridge area. At this spot, the flows of the Charguayacu and Plata rivers have also been collected, reporting values were between 2 to 6.5 m^3/s; the highest values have been observed in December and February and the lowest in August and March with an average of 4.12 m^3/s. The other spots of the river flow show lower values of 2 m^3/s being the upper part of Pindo river the one that reports the lowest values in all the sampling months. Figure 3B shows river flows in tributaries, where one can observe that the highest flows arereported in the Charguayacu tributary in the spots Puente and river mouth. The "Bravo" watercourse

Table 2. Geographical and hydrographic characteristics of the recharge area

	Pindo				Charguayacu		Plata	Bravo
	Upper part	Tributary	Catchment of drinking water	Bridge	Bridge	River mouth	River mouth	River mouth
Ground coverage	Assortment	Secondary forest	Pasture	Assortment	Assortment	Pasture	Relief	Pasture
Distance form Rio Amazonas weather station airport (km)	5.9	5.77	5.24	2.53	4.81	3.22	5.4	2.6
Distance from the Pindo Mirador weather station rain meter (km)	0.3	0.4	3.1	0.1	1.5	2.4	0.4	3
X Coordinate	825201	825185	826098	825200	824224	825538	825236	826163
Y Coordinate	9839427	9839280	9836160	9839112	9838007	9836744	9838791	9836292
max height (m.s.n.m.)				1362		1357	1320	1294
monitoring point height (m.s.n.m.)	1192	1204	1182	1048	1111	1092	1156	1048
Travel distance from last point (km.)	4.19	4.64	0.35	3.03	2.3	5.72	3.23	3.73
Length of accumulated channel (km.)	4.19	4.64	4.99	8.02	2.3	8.02	3.23	3.73
Pending	0.086	0.065	0.078	0.058	0.085	0.06	0.076	0.082
Concentration time (hours)	0.514	0.618	0.609	0.986	0.325	0.972	0.44	0.478
Area of Influence (km^2)	3.43	2.77	6.37	17.3	2.94	4.83	2.99	6.95
Perimeter (km)	7.7	10.7	12.7	18.6	8.3	12.3	7.45	13.6
Coefficient of compactness	1.16	1.75	1.41	1.25	1.36	1.57	1.21	1.45
Elongation ratio	0.8	0.8	0.6	0.8	0.7	0.6	0.6	0.6
Drainage density (km / km)	2.07	2.56	1.73	1.36	1.79	2.275	1.1	0.99
Current density (km)	3.21	5.42	4.08	1.85	3.06	4.47	0.33	2.16

shows a greater variation with flows that oscillate between 0.48 m^3/s in September and 3.93 m^3/s in June with an average of 1.66 m^3/s.

Table 4 shows the statistics of the watercourses, in which Pindo river and metallic bridge are not considered, since these present confluence of other watercourses that have already been reported. With the exception of Plata and Pindo (upper part), the highest flow values have been recorded in the month of June.

Table 5 shows the Pearson correlation analysis between the registered flows and the previous accumulated rainfall, where the distance from the monitoring point to the meteorological station was also calculated. It has also been observed that for all the watercourses the correlation increases more in the previous rainfall accumulated up to 4 days before generates the highest correlation. Also shows the Pearson linear correlation analysis between the flow rate and the coefficient of variation of the flow with the infiltration variables, geographic and meteorological. In this case, it can be seen that the river flow variable shows significant negative correlations at 0.05 in relationship with the accumulated infiltration variables and infiltration speed at 2h and 0.01 including the drainage density, which would indicate that as the infiltration velocity and the drainage density increase, the flow rate decreases. The same table also shows that the flow has positive correlations at 0.05 with the compactness coefficient variables and the previous accumulated rainfall on days 4 and 5.

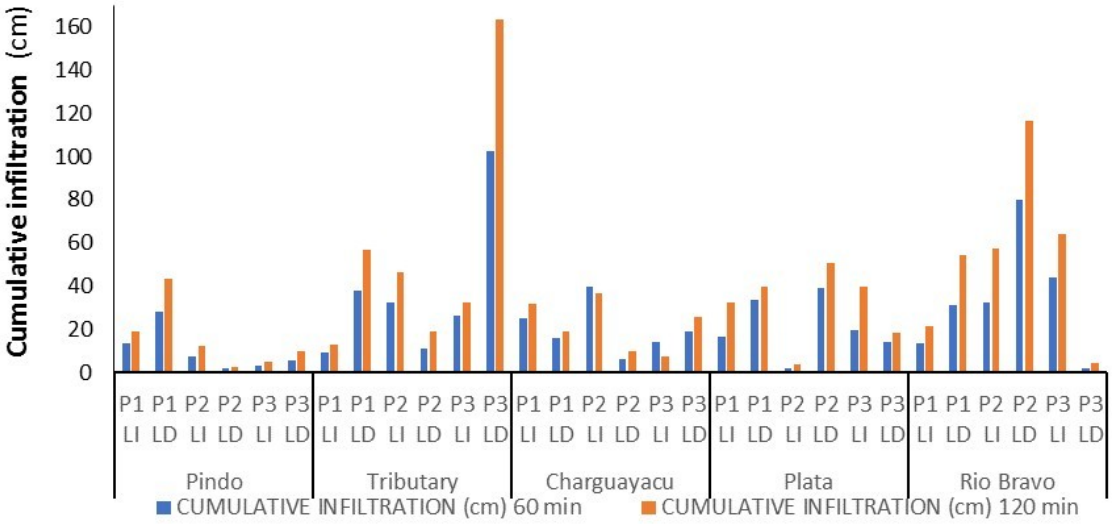

Figure 2. Cumulative infiltration at 1h and 2h

Table 3. Statistics for 1h and 2h speeds of the corresponding water courses

River	Rainfall (over the last 5 days)	Previous humidity condition	Time (hours)	Average (cm/h)	S.D.	C.V ,	Min.	Max.
Pindo	120	III	1h	10	9.7	97.2	1.9	28.1
			2h	7.7	7.5	97.4	1.3	21.7
Unnamed Tributary	108,1	III	1h	36.6	34.3	93.7	9.3	102.7
			2h	27.5	27.7	100.6	6.5	81.6
Bravo	3,56	I	1h	33.8	27.1	80.0	1.9	79.9
			2h	26.4	19.4	73.4	2.1	58.1
Charguayacu	3,56	I	1h	20.1	11.4	56.3	6.5	39.6
			2h	10.9	5.8	53.4	3.9	18.3
Plata	7,37	I	1h	20.7	13.5	65.5	1.8	38.9
			2h	15.4	8.5	55.2	1.8	25.4

S.D. standard deviation C.V. coefficient of variation

This demonstrates that with a compactness index close to 1 they will report lower flows, which indicates that circular basins with values close to one present higher flood risks according to the interpretation of the index value (Askoa, 2004). Being areas within the same hydrographic system, a recharge zone with a lower coefficient of compactness is longer in relation to the same area and therefore it has a longer course of the main course increasing its flow for the area conditions where average annual precipitations above 5000 mm take place. It also shows significant correlations at 0.01 with the area of the basin. Being rivers surrounded by mountains, we could say that more influence means more collection area and therefore greater flow.

The analysis of variance (Table 6) of the type of infiltration, coverage and the coefficient of variation of the flow reported significant differences for the p value <0.001 in the four variables evaluated. The Duncan´s mean comparison test (Table 6) reported the infiltration variables for the regenerated forest and mosaic coverage, as well as the highest values for the infiltration velocity measurements at 1 and 2 hours and the cumulative infiltration at 2h, but they are also the ones that report the greatest flow variability, which could be due to the fact that in these areas the water is not

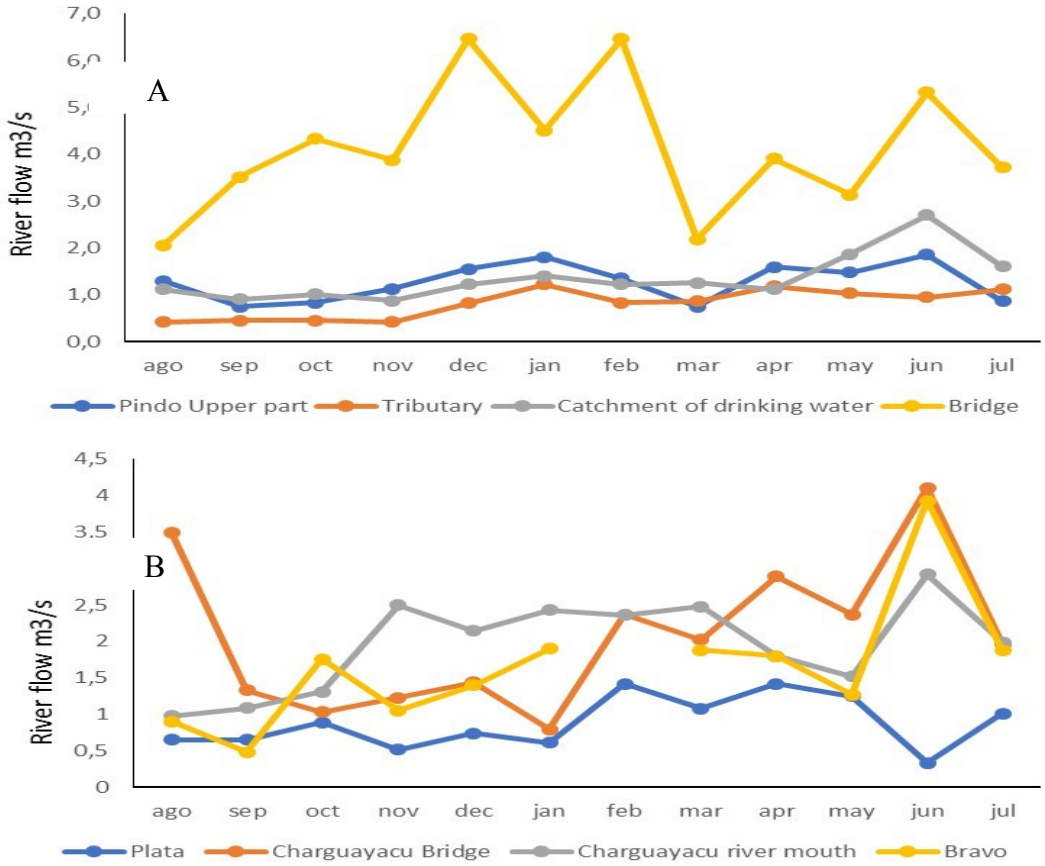

Figure 3. River flow a) Pindo b)Tributaries

Table 4. Statistics of the flow measurement

River	Pindo		Tributary		Bravo		Charguayacu		Plata	
Rainfall (last 5 days) (mm)	120		108.1		3.56		3.56		7.37	
Previous humidity condition	III		III		I		I		I	
RIVER FLOW (m3/s)										
Average (m3/s)	1.27		0.81		1.66		1.96		0.88	
D.E.	0.4		0.31		0.89		0.62		0.36	
CV	31.67		37.76		53.6		31.84		40.75	
Min	0.75		0.42		0.48		0.98		0.33	
Max	1.86		1.22		3.93		2.92		1.42	
1 day	0.26		-0.002		0.24		0.31		0.04	
2 days	0.5		0.3		0.16		0.45		0.22	
3 days	0.53		0.34		0.35		0.3		0.4	
4 days	0.55		0.51		0.21		0.26		0.48	
5 days	0.52		0.49		0.21		0.25		0.5	
	Infiltration rate									
Time (hours)	1h	2h	1h	2h	1h	2h	1h	2h	1h	2h
Average	10	7.7	36.6	27.5	33.8	26.4	20.1	10.9	20.7	15.4
D.E.	9.7	7.5	34.3	27.7	27.1	19.4	11.4	5.8	13.5	8.5
CV	97.2	97.4	93.7	100.6	80	73.4	56.3	53.4	65.5	55.2
Min	1.9	1.3	9.3	6.5	1.9	2.1	6.5	3.9	1.8	1.8
Max	28.1	21.7	102.7	81.6	79.9	58.1	39.6	18.3	38.9	25.4

Table 5. Pearson's linear correlation analysis

	Measurement	River flow (m^3/s)	Coefficient of river flow variation
Infiltration	Infiltration rate in 1 h (cm/h)	-0.121	.527**
	Accumulated infiltration 2H (cm.)	-.237*	.506**
	Infiltration speed 2h (cm/h)	-.237*	.506**
Geographic characteristics	Area (km^2)	.336**	.328**
	Channel length (km)	-0.051	-.686**
	Coefficient of compactness	.252*	-.386**
	Drainage density (km channel / km^2)	-.334**	-0.172
	Current density (No of currents / km^2)	0.229	-.275*
Precipitation conditions	Previous rainfall accumulated 4 days (mm)	.273*	3.76 E-18
	Previous rainfall accumulated 5 days	.255*	-1.19 E-18

* Significant correlation to 0.05 ** Significant correlation to 0.01

Table 6. Variance analysis and average comparison test of the soil cover type factor with infiltration variables and the flow variation coefficient.

Parameter	P value	Error
Infiltration rate at 1 hour	<0.0001	35.18
Cumulative infiltration in 2h	<0.0001	123.3
Infiltration Speed 2h	<0.0001	30.83
Coefficient of caudal variation	<0.0001	2.76
Average comparison test		
Parameter	Coverage	Average
Infiltration speed 1h (cm / h)	Regenerated forest	28.65 a
	Mosaic	27.82 a
	Grass	20.13 b
	Secondary forest	10.00 c
Accumulated infiltration 2h (cm)	Regenerated forest	42.92 a
	Mosaic	38.60 a
	Grass	21.78 b
	Secondary forest	15.30 b
Infiltration speed 2h (cm / h)	Regenerated forest	21.46 a
	Mosaic	19.30 a
	Grass	10.89 b
	Secondary forest	7.65 b
Variability of the flow rate (cm / h)	Secondary forest	31.67 a
	Grass	31.84 a
	Regenerated forest	39.26 b
	Mosaic	51.24 c

a, b, c values with common letters do not differ for $P < 0.05$

stored in the subsurface layers of the soil that would feed the adjacent watercourses, but most of it would infiltrate through deep percolation towards underground flows.

The records of maximum rainfall were analyzed in a 24h period at the meteorological station in Rio Amazonas airport from 1981 to 2017, (Figure 4). It can be identified that in a period of 37 years, 40.5% of these years reported values between 100 and 125 mm/24h, while 21.6% of them reported values higher than 150mm/24h. Extreme events show intensities of 179.8mm and the last event recorded in 2016 shows 171.4mm. A tendency to decrease of the sheets in 24h in extreme events is identified as shown by the trend line. The analysis of maximum precipitations shows that June and November are the months with the highest number of maximum rainfall events in a 24 hour period per year. July, on the other hand, didn't report any events of maximum precipitation in the same period of time.

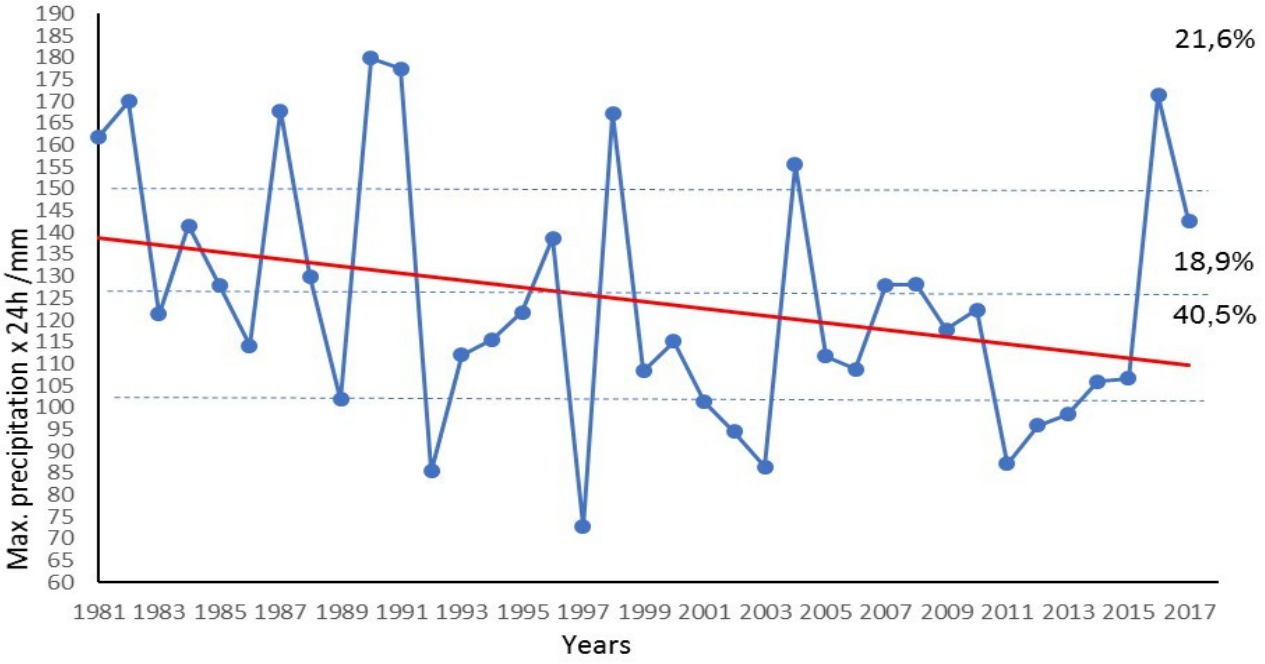

Figure 4. Maximum rainfall / 24h period 1981-2017

For the flood modeling in the hyetograph design (Figure 5 A) the last large flood event recorded between December 29th and 30th, 2016 was considered. An accumulated rainfall was recorded between 5:00 pm and 08:00 am on that date (244.6mm) registering the maximum precipitation at 0:00 am with an intensity of 86.6 mm/h.

Based on the characteristics of minimum infiltration rate, presence of humus, and litter height and having a previous accumulated rainfall in the 5 days prior to the event of 43.6 mm and an initial abstraction of 60, the NC curve number was determined. As proposed by Gaspary et al., (2003) in condition 2 following data was obtained: Rio Pindo 16, tributary (no name) 17.5; Rio Charguayacu 45, Rio Plata 55 and Rio Bravo 45.

With these parameters and the characteristics of the areas of influence, the modeling was carried out using the HEC-HMS program for the establishment of the complete hydrograph considering 2 conditions. Firstly, the flood without loss model (Figure 5 C). In this case, the Pindo spot "metal bridge" reaches a maximum value of 216.94 m3/s. Secondly, the flood with loss model (Figure 5B) reaches a maximum value of 26.71 m3/s. Measurements taken some days after the flood, at a spot located 1.5 km downstream from Pindo-metal-bridge (that does not receive more water from other tributaries) allowed to do an estimation following the flood marks left on the ground.

The data obtained here were the following: a slope of 1%; average wet area 67.35m^2; exit area 80.84m2; height of flood 3m; perimeter of wet soil 56.75m; base expense 2.6m3/s. Applying the formula of Manning a flood flow of 226.96 m^3/s was established which indicates that the lossless model is closer to the value estimated by the flood footprint. These characteristics could have happenedin order to surpass the initial abstraction capacity (Aroca, 2014) of the previous days with a cumulative 5-day rainfall of 14 mm. If we add it the previous precipitation in the last hours (127.4mm) it could have generated a saturation of the soil in the upper part of the river, where the accumulated infiltration in 2 hours averaged a rate of 15.3 cm.

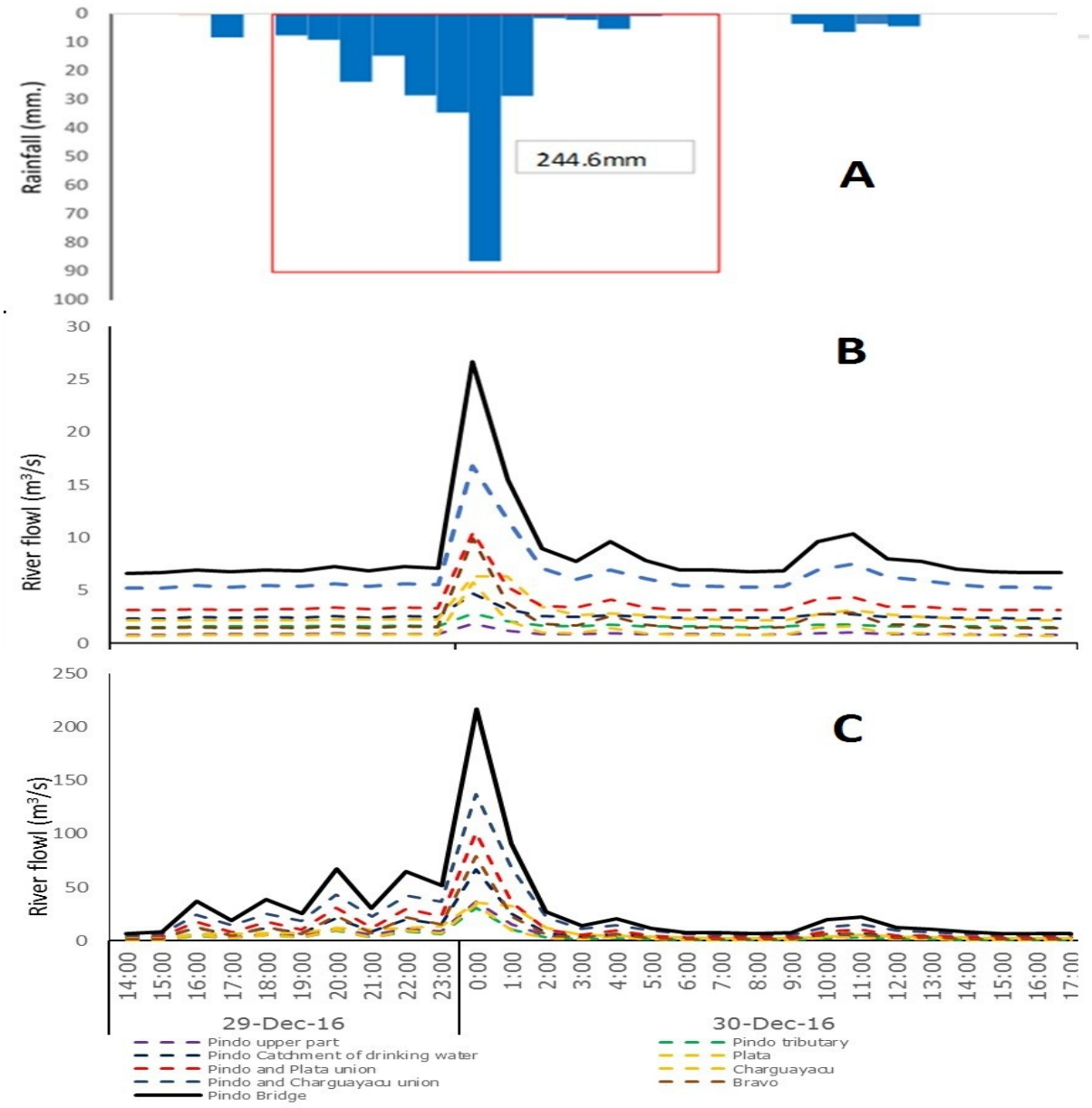

Figure 5. Complete Hydrograph: A) Hyetograph B) Hydrograph with loss model C) Hydrograph without loss model

DISCUSSION

According to Meza, (2014) the Rio Pindo & tributary as well as the metallic bridge and Rio Plata present coefficients of compactness between 1 and 1.25 which are considered as round basins. The Bravo course is considered round oval to oval elongated and the Charguayacu river has an oblong oval to rectangular oblong form. The same author also states that in terms of drainage density, values greater than 0.5 indicate efficiency in drainage, while Camino et al. (2018) suggests that basins with values between 1 and 1.25 are considered as almost round to round oval and that these basins present greater danger of floods due to their relative equidistance from the points located in the watershed with respect to a central one.

According to Breña and Jacobo (2006) all the watercourses correspond to pronounced dependent basins in terms of the elongation relationship.

The enhancement coverage has a higher infiltration rate for both 1 hour and 2 hours, unlike a secondary forest that has a lower infiltration rate and a lower flow variability. This is because the vegetation cover which consists of trees, shrubs and grasses that regulate the amount of flow in the stream in primary and secondary forests (González et al., 2016). A mosaic, on the other hand, presents greater flow variability due to the scarce presence of vegetation cover and shows a low infiltration speed, which produces run-off that goes to the channel increasing the flow as it mentions Valero et al. (2003) who indicates that a change in the vegetation cover directly influences the Hydrological response of the basins during the rain events. García et al., (2011) states that the coverage and land use affect the continental hydrological cycle, where the canopy fulfills functions in interception, evapotranspiration, infiltration and regulation of runoff generated in storms.

As seen in Figure 5, the precipitation influences the increase in flow because the estimated response time in terms of the concentration time does not exceed 1h. This generates an immediate response, which is influenced by the morphological characteristics of the basin. Méndez & Marcucci, (2006), indicate that the slope and density of drainage influence the time of concentration of the micro basin of the Curucutí creek. As a result, there is a longer concentration time due to the characteristics of the basin that showed an average drainage density that captures the highest concentration of runoff. Caballero (2011) states that in mountain areas the risk of torrential floods is high depending on the length of the basin, slope and contributing materia.

CONCLUSIONS

The water courses that feed the Pindo River showed the following characteristics like areas with less than 10 km^2 area and river channels lengths of up to 8 km. Most of them, due to their slope, are considered as mountain courses with high slopes greater than 7%. The tributary courses and Bravo are those that have compactness coefficients closer to unity and therefore have a higher risk of flooding. With the exception of the Bravo river, all the other water courses have a high drainage density. Four land uses were presented, where soils with enhanced forest show a higher infiltration rate and those covered by forest show less variability in flow. The geographical characteristics influence the flow and the infiltration on the variability. In flood conditions, applying the SCS model, the flow behavior estimated by the water footprint method is more similar to a lossless model than to a loss model, reaching 216 m^3/s. The area reports high precipitations, but the tendency to the presence of extreme events has decreased in the last decades, and the curves of intensity duration and frequency show intensities that can surpass 60 mm/h in periods of 2 and 5 years.

ACKNOWLEDGEMENTS

We would like to thank Henry Navarrete from the Geographic Information Systems Department of the Amazon State University, Fabricio Ríos, Rodrigo Haro and all the authorities from the Environmental Management Direction of the Provincial Autonomous Decentralized Government of Pastaza. Without all their support, this research project could not have been carried out.

REFERENCES

Abril, R. 2012. Estudio de impacto ambiental ex post en dique del rio pindo en Shell cantón Mera. Disertación de Maestría, Escuela Superior Politécnica del del Ejercito (ESPE), Sangolquí, Ecuador, 2012.

Aroca, E. 2014. Importancia de las abstracciones iniciales para la génesis de avenidas en cuencas de montaña. Disertación de Masterado, Universidad de Cantabria, España.

Askoa, I. 2004. Análisis morfométrico de la cuenca y Red de Drenaje del río Zadorra y sus afluentes aplicado a la peligrosidad de crecidas. Boletín de la Asociación de Geógrafos Españoles., vol .38, pp. 311-329

Argañaraz, J., and Lorenz, G. 2010. Contribución de las áreas verdes urbanas a la regulación del balance de agua en Santiago del Estero, Argentina. Bosque (Valdivia)., Vol. 31 (3), pp. 231-242

Blanco, R. 1999. El Infiltrómetro de cilindro simple como método de cálculo de la conductividad hidráulica de suelos. Experiencias de campo en ámbitos de montañas mediterráneas. Baetica. Estudios de Arte, Geografía e Historia., Vol. 21. pp. 21. 9-33.

Breña, A., and Jacobo. N., 2006. Principios y Fundamentos de la Hidrología Superficial. México; Universidad Autónoma Metropolitana.

Caballero. J. 2011. Las avenidas torrenciales una amenaza potencial en el valle de Aburrá. Revista Gestión y Ambiente., Vol 14(3). pp. 45-50

Camino, M., Bo, M., Cionchi, J. Lopez de Armentia, J., Del Rios,J. and De Marco, S. 2018. Estudio morfométrico de las cuencas de drenaje de la vertiente sur del sudeste de la provincia de Buenos Aires (Argentina). Revista Universitaria de geografía., Vol. 27 (1) pp. 73-97

Chow V., Maidment D., and Mays L.2013. Applied Hydrology. New York; McGraw-Hill.

Colmenares, G., Segura, F., Pardo, J., Ruiz, L., and Palomar, J. 2013. Estimación De La Velocidad Del Flujo Del Agua En Cauces Efímeros No Aforados A Partir De Datos Lidar Y Gps-Rtk. Boletín de la Asociación de Geógrafos Españoles., Vol. 62, pp. 7-23

Conesa, C. and García, R., 2011ª. Factores e Índices de peligrosidad de las aguas de avenida en cruces de carreteras con ramblas. Estudio aplicado a la vertiente litoral sur de la región de Murcia. Boletín de la Asociación de Geógrafos Españoles. Vol., 57, pp.195-218

Conesa, C., and García, R., 2011b. Estimación de caudales de avenidas y delimitación de áreas inundables mediante métodos hidrometeorológicos e hidráulicos y técnicas S.I.G., estudio aplicado al litoral sur de la región de Murcia. Papeles de Geografía., Vol.53-54, pp. 107-123

Di Rienzo J., Casanoves, F., Balzarini, M., Gonzalez, L., Tablada, M., and Robledo,C. 2014. INFOSTAT, Grupo INFOSTAT, FCA, Universidad Nacional de Córdoba, Argentina,.

García, J., López, I., Vicente, S., Lasanta, T., and Begueira, S. 2011. Mediterranean water resources in a global change scenario. Earth-Science Reviews. Vol.,105 (3,4), pp.121-139.

Garzón, M., Ortega, J., and Garrote, J. 2009. Las Avenidas Torrenciales En Cauces Efímeros: Ramblas Y Abanicos Aluviales. Enseñanza de las Ciencias de la Tierra. Vol. 17 (3), pp. 264-276

Gaspari, F., Rodríguez, A., Senisterra, G., Delgado, M., and Besteiro, S. 2013. Elementos metodológicos para el manejo de cuencas hidrográficas. Buenos Aires Argentina Editorial de la Universidad de la Plata.,.

González, A.. Álvarez, P., González, M., and Aguirre, Z. 2016. Influencia de la cobertura vegetal en los coeficientes de escorrentía de la cuenca del río Catamayo, Ecuador., Ecuador. CEDAMAZ., Vol. 6, pp.50-59

Helton, A., Poole, G., Payn, R., Izurieta, C., and Stanfordd, J. 2014, Relative influences of the river channel, floodplain surface, and alluvial aquifer on simulated hydrologic residence time in a montane river floodplain. Geomorphology., Vol. 205, pp.17-26

IBM, International Business Machine. SPSS Statistic, 2013.

López, R., and Barragán, J. 2004. Desarrollo de ecuaciones de flujo uniforme para ríos de grava. Ingeniería Civil., Vol. 135, pp. 95–102.

Méndez, W., and Marcucci, E. 2006. Análisis morfométrico de la microcuenca de la quebrada Curucutí, estado Vargas-Venezuela. Revista Geográfica Venezolana., Vol. 47 (1), pp. 29-55.

Meza, M., Rodríguez, A., Corvacho, O., and Tapia, A. 2014. Análisis morfométrico de microcuencas afectadas por flujos de detritos bajo precipitación intensa en la quebrada de Camiña, norte grande de Chile. Diálogo andino., Vol. 44, pp. 15-24.

Pérez, P., Zema, M., Vente, D., and Boix, C. 2018. Efectos de la revegetación a escala de cuenca sobre el caudal y la evapotranspiración en ambiente mediterráneo. Cuenca del Taibilla (SE de España). Bosque (Valdivia)., Vol. 39 (1), pp. 119-129.

Pizarro, T., Soto, B., Farias, D., and Jordan, D. 2005. Aplicación de dos Modelos de Simulación Integral Hidrológica, para la estimación de caudales medios mensuales, en dos cuencas de Chile central. Bosque (Valdivia)., Vol. 26 pp. 123-129.

Ren, L., Yuan, F., Yong, B., Jian., S., Yang, S., Gong, L., Ma, M., Liu, Yi., and Shen, Y. 2014, Where does blue water go in the semi-arid area of northern China under changing environments?, Evolving Water Resources Systems: Understanding, Predicting and Managing Water–Society Interactions proceedings of ICWRS2014, Bologna, Italy., Vol. 364 pp. 88-93.

Ruiz, R., and Torres, H. 2008. Manual de procedimientos de delimitación y codificación de unidades hidrográficas, uicn sur SGCAN Unión Internacional para la Conservación de la Naturaleza (UICN).

U.S. Army Corps of Engineers Institute For Water Resources Hydrologic Engineering Center 2017 HEC-HMS vers 4.2.1

Valero, V., López, J.., García, J., and Begueira, S. 2003. Intensidad de las avenidas y aterramiento de embalses en el Pirineo Central español, Erìa., Vol. 61 pp. 159-167

Villavicencio, R., García, R., Martínez, R., Toldeo, S. Guevara, R y Ávila, R. 2014. Infiltración de agua y medición del caudal de arroyos en la sierra de Quila. Revista. Mexicana. De Ciencias. Forestales., Vol. 5 (24), pp.184-201

Sun, X.., Bernard, L., Garneau, C. Volk, M. Arnold, J., Srinivasan, R. Sauvage, s. Sánchez, J.2015. Improved simulation of river water and groundwater exchange in an alluvial plain using the SWAT model. Hydrological Processes., Vol. 30 (2) pp. 187-202.

ADDRESS FOR CORRESPONDENCE
Ricardo Abril
Departamento de Ciencias de la Vida
Universidad Estatal Amazónica
Km 2 ½ Vía a Napo
Pastaza, Ecuador
Email: rvabril@uea.edu.ec.